# Fourier Ptychographic Imaging

A MATLAB® tutorial

**Online at: https://doi.org/10.1088/978-1-6817-4273-1**

# Fourier Ptychographic Imaging

A MATLAB® tutorial

**Guoan Zheng**
*University of Connecticut, Storrs, CT, USA*

Morgan & Claypool Publishers

ISBN 978-1-6817-4273-1 (ebook)
ISBN 978-1-6817-4272-4 (print)
ISBN 978-1-6817-4275-5 (mobi)

DOI 10.1088/978-1-6817-4273-1

Version: 20160501

IOP Concise Physics
ISSN 2053-2571 (online)
ISSN 2054-7307 (print)

A Morgan & Claypool publication as part of IOP Concise Physics
Published by Morgan & Claypool Publishers, 40 Oak Drive, San Rafael, CA, 94903, USA

IOP Publishing, Temple Circus, Temple Way, Bristol BS1 6HG, UK

*To my family for all their love and support*

# Contents

# Preface

Fourier ptychography is a new imaging technique that bypasses the resolution limit of the employed optics. In particular, it transforms the general challenge of high-throughput, high-resolution imaging from one that is coupled to the physical limitations of the optics to one that is solvable through computation. This book began as a collection of lecture notes and MATLAB® simulation examples on the Fourier ptychography technique. In teaching this technique in a graduate course, I found that the students were able to develop a better conceptual understanding using simulation examples. Following the same line of reasoning, this book demonstrates the concept of Fourier ptychography in a tutorial form and provides many MATLAB simulation examples for the reader. It also discusses the experimental implementation and recent developments of the technique. This book will be of interest to researchers and engineers learning simulation techniques for Fourier optics and the Fourier ptychography concept.

The book begins in chapter 1 with a short review of imaging concepts in Fourier optics. It provides simulation examples on coherent and incoherent imaging systems. It also covers the modeling of Zernike aberrations in imaging systems.

Chapter 2 covers the imaging procedures of the Fourier ptychography technique. In particular, it provides simulation examples on the forward imaging model, the iterative recovery process, and the aberration-correction scheme. It also discusses the sampling requirement, the optimal updating order, and the decomposition of state-mixture in Fourier ptychography.

Chapter 3 covers different experimental implementations of the Fourier ptychography technique, including the LED-array approach, the liquid-crystal-display approach, and the aperture-scanning implementation. It also discusses different coherent imaging modalities using Fourier ptychography, including bright-field, dark-field, phase, phase-gradient, reflective, and multi-slice imaging.

Chapter 4 extends the Fourier ptychography framework to incoherent imaging settings. It provides simulation examples on the pattern-illuminated Fourier ptychography scheme. It also covers the 4-frame resolution-doubling scheme and the multiplexed structured illumination approach.

Chapter 5 summarizes the book and provides the directions for future developments.

For more information on the Fourier ptychography technology, please refer to Smart Imaging Lab @ UConn: https://sites.google.com/site/gazheng/.

Guoan Zheng
December 2015

# Acknowledgements

I would like to thank my students Siyuan Dong and Kaikai Guo for their developments of some simulation examples in this book. I would also like to thank Professor Changhuei Yang, Professor Rongguang Liang, Professor Charles DiMarzio, Dr Roarke Horstmeyer, and Dr Xiaoze Ou for their helpful discussions over the past few years. The development of the Fourier ptychography technology in my lab is currently supported by NSF CBET 1510077. Lastly and most importantly, I want to express my gratitude to my wife and my parents. I could not have finished this book without their unconditional support.

# Author biography

## Guoan Zheng

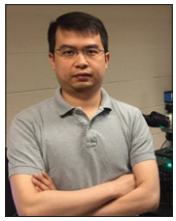

Dr Guoan Zheng is an Assistant Professor at University of Connecticut, with a joint appointment from the Biomedical Engineering Department and the Electrical Engineering Department. His primary field of expertise lies in microscopy, optical engineering, biophotonics, computational imaging, and lab-on-a-chip devices. His current research interests include Fourier ptychography, high-throughput imaging technologies, super-resolution imaging, phase retrieval techniques, and the development of optofluidics and chip-scale imaging solutions. He earned his MSc and PhD in Electrical Engineering from Caltech. He received the $30 000 Lemelson-MIT Caltech Student Prize in 2011 for his development of chip-scale microscopy solutions. He got the Caltech Demetriades Thesis Prize in 2013 for his development of the Fourier ptychography technology. His research has resulted in more than 50 peer-reviewed publications and 15 issued/pending patents, four of which have been extensively reported and highlighted by national media agencies.

**IOP** Concise Physics

Fourier Ptychographic Imaging

A MATLAB® tutorial

**Guoan Zheng**

# Chapter 1

## Basic concepts in Fourier optics

In this chapter, we will briefly review the basic concepts in Fourier optics. The operation of conventional imaging systems can be modeled by two steps, as shown in figure 1.1: 1) the low-pass filtering process of the imaging system, and 2) the discrete sampling process of the image sensor.

In step 1, the employed optical system acts like a low-pass filter, with a cutoff frequency determined by the numerical aperture (NA) of the lens. Only the spatial-frequency components within the passband can be collected by the optical system and form an image at the detector plane. Such a low-pass filtering process imposes a resolution limit on the imaging platform. For coherent imaging, the resolution limit for the complex light field is $\lambda$/NA, where $\lambda$ is the wavelength of the incident light. For incoherent imaging, the resolution limit for the intensity signal is $\lambda/(2\text{NA})$.

In step 2, the light signal is sampled by the image sensor. The pixel size of the image sensor needs to satisfy the Nyquist limit, i.e., at least two samples are made for the smallest feature of the signal. If the pixel size of the image sensor is too large, it would introduce the aliasing problem to the final captured image, as shown in figure 1.1 (bottom right). A smaller pixel size of the image sensor helps to address the aliasing problem; however, it may also impose limitations on the dynamic range and the signal-to-noise ratio of the sensor chip.

In the following, we will discuss the coherent and incoherent imaging systems from the transfer-function point of view. We will also discuss how to model optical aberrations in imaging systems. Materials in this chapter are useful for understanding the concept of Fourier ptychography (FP). The interested reader can also refer to [1–3] for more details on Fourier optics.

### 1.1 Coherent imaging system

We first consider a coherent imaging system where a spatially coherent light source is used for sample illumination (we will refer to it as coherent illumination in the future). Under coherent illumination condition, the phasor amplitudes of the light

doi:10.1088/978-1-6817-4273-1ch1

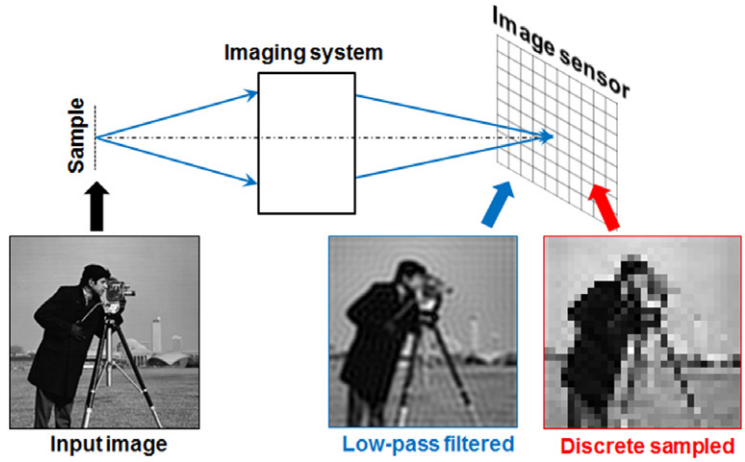


**Figure 1.1.** The operation of conventional imaging systems. The light field from the object (bottom left) is low-pass filtered by the imaging system (bottom middle) and discretely sampled by the image sensor (bottom right).

field vary in unison at all spatial points. Therefore, a coherent imaging system is linear in complex amplitude:

$$A_{\text{output}}(x, y) = h(x, y) \otimes A_{\text{input}}(x, y) \tag{1.1}$$

In equation (1.1), $A_{\text{input}}$ and $A_{\text{output}}$ represent the input and output complex amplitudes of the light field, $h(x, y)$ represents the coherent point spread function in the spatial domain, and '$\otimes$' represents 2D convolution. We can transform equation (1.1) to the spatial-frequency (Fourier) domain and obtain:

$$G_{\text{coh\_output}}\left(k_x, k_y\right) = H_{\text{coh}}\left(k_x, k_y\right) G_{\text{coh\_input}}\left(k_x, k_y\right) \tag{1.2}$$

In equation (1.2), $G_{\text{coh\_input}}$ and $G_{\text{coh\_output}}$ represent the input and output Fourier spectrums of the complex amplitudes. $H_{\text{coh}}(k_x, k_y)$ is the Fourier transform of $h(x, y)$ and it is commonly referred to as coherent transfer function.

Coherent illumination condition can be obtained when the light waves come from a single point source. The common light sources for coherent illumination are laser diodes and spatially-confined LEDs. We can also add a small pinhole in front of an extended light source to obtain the coherent illumination condition (the pinhole can be treated as a single point source in this case). In this case, however, the achievable brightness would be much weaker than the case of laser diode. Strictly speaking, there is no real point source for coherent illumination; even for laser diode, the light emitting area has a certain size. Rigorous treatment of the coherent illumination condition is beyond the scope of this book. The interested reader can refer to the theory of partial coherence in [2].

To simulate the imaging process of a coherent imaging system, we consider a microscope example with a 1× magnification, 0.2 NA objective lens. The incident wavelength is 0.5 μm and the final image is sampled by an image sensor with a 0.5 μm pixel size. In the following, we will first create a high-resolution input object

(lines 1–4) and set up the coherent imaging system (lines 5–9). We will then simulate the low-pass filtering process of the imaging system (lines 10–21). Finally, we will obtain the output complex amplitude and intensity images of the simulated object (lines 22–26).

```
1   %% simulate a high-resolution object
2   objectIntensity = double(imread('cameraman.tif'));
3   objectAmplitude = sqrt(objectIntensity);
4   imshow(objectAmptitude,[]);title('Input object (amplitude)');
5   %% set up the parameters for the coherent imaging system
6   waveLength = 0.5e-6;
7   k0=2*pi/waveLength;
8   pixelSize = 0.5e-6;
9   NA = 0.1; cutoffFrequence = NA*k0;
10   %% set up the low-pass filter
11   objectAmptitudeFT=fftshift(fft2(objectAmptitude));
12   [m n]=size(objectAmptitude);
13   kx=-pi/pixelSize:2*pi/(pixelSize*(n-1)):pi/pixelSize;
14   ky=-pi/pixelSize:2*pi/(pixelSize*(n-1)):pi/pixelSize;
15   [kxm kym]=meshgrid(kx,ky);
16   CTF=((kxm.^2+kym.^2)<cutoffFrequency^2); % the coherent transfer function
17   imshow(CTF,[]);title('CTF in the spatial frequency domain');
18   %% the filtering process
19   outputFT=CTF.*objectAmptitudeFT;
20   imshow(log(abs(outputFT)),[]);
21   title('Filtered spectrum in the spatial frequency domain');
22   %% output amplitude and intensity
23   outputAmplitude = ifft2(ifftshift(outputFT));
24   outputIntensity = abs(outputAmplitude).^2;
25   figure;imshow(outputAmplitude,[]);
26   title('Output object (amplitude)');
```

In line 2, we simulate a high-resolution intensity object. We assume the phase of the object is a constant and we convert the intensity to complex amplitude in line 3. In lines 5–9, we set up the parameters for the coherent imaging system. In particular, we define the wave number in line 7 and the cutoff frequency in line 9. In lines 11–17, we set up the low-pass filter (i.e. the coherent transfer function) in the spatial-frequency domain. The low-pass filtering process is performed in line 19, where we transform the object's complex amplitude to the spatial-frequency domain using fast Fourier transform and multiply it with the coherent transfer function. The filtered spectrum is then transformed back to the spatial domain using the inverse fast Fourier transform in line 23. The final output amplitude and intensity can be obtained in lines 23 and 24.

The results of this simulation study are shown in figure 1.2, where we compare the input and output amplitude in both the spatial and spatial-frequency domains (spatial-frequency domain will be referred to as Fourier domain in the future). We note that, a coherent imaging system is linear in complex amplitude, and thus, the filtering process in line 19 is for the complex amplitude of the light field, not the intensity. Once we obtain the output complex amplitude, we can convert it back to intensity, as shown in line 24. We also note that, conventional image sensors can only detect light intensity; the complex phase information is lost in the measuring process. In order to detect the complex amplitude information, we can use phase retrieval [4–12] or holographic approaches [13–15] to recover the lost phase information from intensity measurements. In particular, Fourier ptychography is

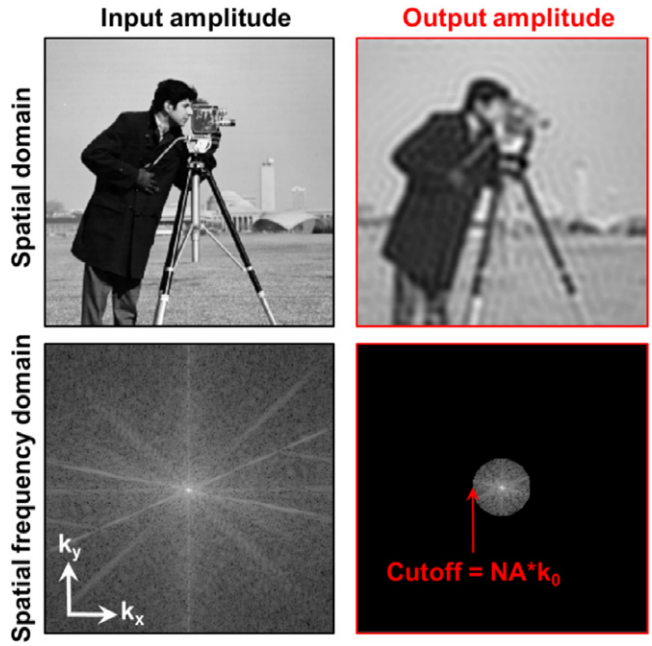


**Figure 1.2.** The low-pass filtering process of a coherent imaging system.

a coherent phase-retrieval approach. In the recovery process of FP, the acquired intensity images under different incident angles are used to recover the complex amplitude of the object and improve the resolution beyond the cutoff frequency of the employed optics [16].

## 1.2 Incoherent imaging system

In a coherent imaging system, the illumination light waves come from a point source and the phasor amplitudes of the light waves vary in unison at all spatial points. Here, we consider another illumination condition with the opposite property such that the phasor amplitudes at different points vary in a totally uncorrelated manner. Such an illumination condition is called spatially incoherent (we will simply refer to it as incoherent in the future). The most common example for incoherent imaging is the Köhler illumination in microscope settings, where samples are illuminated by uncorrelated plane waves from different incident angles.

For an incoherent imaging system, the impulse responses at different spatial points vary in an uncorrelated manner. As such, they must be added on an intensity basis instead of the complex amplitude basis. It follows that an incoherent imaging system is linear in intensity and the point spread function is the squared magnitude of the coherent point spread function:

$$I_{\text{output}}(x, y) = |h(x, y)|^2 \otimes I_{\text{input}}(x, y) \tag{1.3}$$

In equation (1.3), $I_{\text{input}}$ and $I_{\text{output}}$ represent the input and output intensity images, and $h(x, y)$ is the coherent point spread function in the spatial domain. The impulse

response $|h(k_x, k_y)|^2$ is commonly known as incoherent point spread function. We can also transform equation (1.3) to the Fourier domain and obtain:

$$G_{\text{incoh\_output}}(k_x, k_y) = H_{\text{incoh}}(k_x, k_y) G_{\text{incoh\_input}}(k_x, k_y) \tag{1.4}$$

In equation (1.4), $G_{\text{incoh\_input}}$ and $G_{\text{incoh\_output}}$ represent the input and output Fourier spectrums of the intensity images, and $H(k_x, k_y)$ is the Fourier transform of $|h(x, y)|^2$ and known as incoherent transfer function.

In the following, we will use the same microscope imaging example (1× magnification, 0.1 NA objective lens, 0.5 μm wavelength, and 0.5 μm pixel size) to demonstrate the incoherent imaging process. The key idea of this simulation is to generate the incoherent transfer function and perform the low-pass filtering process in the Fourier domain.

```
1   %% simulate an incoherent imaging system
2   objectIntensity=double(imread('cameraman.tif'));
3   imshow(objectIntensity,[]);title('Input object (intensity)');
4   %% set up the parameters for the coherent imaging system
5   waveLength = 0.5e-6;
6   k0=2*pi/waveLength;
7   pixelSize = 0.5e-6;
8   NA = 0.1;
9   cutoffFrequency = NA*k0;
10  %% set up the coherent transfer function in the Fourier domain
11  objectIntensityFT=fftshift(fft2(objectIntensity));
12  [m n]=size(objectIntensity);
13  kx=-pi/pixelSize:2*pi/(pixelSize*(n-1)):pi/pixelSize;
14  ky=-pi/pixelSize:2*pi/(pixelSize*(n-1)):pi/pixelSize;
15  [kxm kym]=meshgrid(kx,ky);
16  CTF=((kxm.^2+kym.^2)<cutoffFrequency^2); % pupil function circ(kmax)
17  imshow(CTF,[]);title('Coherent transfer function in the Fourier domain');
18  %% set up the incoherent transfer function
19  cpsf=fftshift(ifft2(ifftshift(CTF))); % coherent PSF
20  ipsf=(abs(cpsf)).^2; % incoherent PSF
21  OTF=abs(fftshift(fft2(ifftshift(ipsf)))); % incoherent transfer function
22  OTF=OTF./max(max(OTF));
23  figure;imshow(abs(OTF),[]);
24  title('Incoherent transfer function in the Fourier domain');
25  %% perform low-pass filtering and generate the output intensity image
26  outputFT=OTF.*objectIntensityFT;
27  imshow(log(abs(objectIntensityFT)),[]);
28  title('Filtered spectrum in the Fourier domain');
29  outputIntensity = ifft2(ifftshift(outputFT));
30  figure;imshow(outputIntensity,[]);title('Output object (intensity)');
```

Similar to the coherent imaging case, we generate the coherent transfer function in line 16. We then transform the coherent transfer function to the spatial domain and obtain the coherent point spread function in line 19. Next, we take the squared magnitude of the coherent point spread function to obtain the incoherent point spread function in line 20. Finally, we transform the incoherent point spread function back to the Fourier domain to obtain the incoherent transfer function in line 21. The low-pass filtering process is performed in line 26, similar to the case of coherent imaging. The final low-pass filtered intensity output is obtained in line 29 and it is shown in figure 1.3.

Figure 1.4 shows the comparison between the coherent and incoherent transfer functions. We can see that the cutoff frequency of the incoherent transfer function is

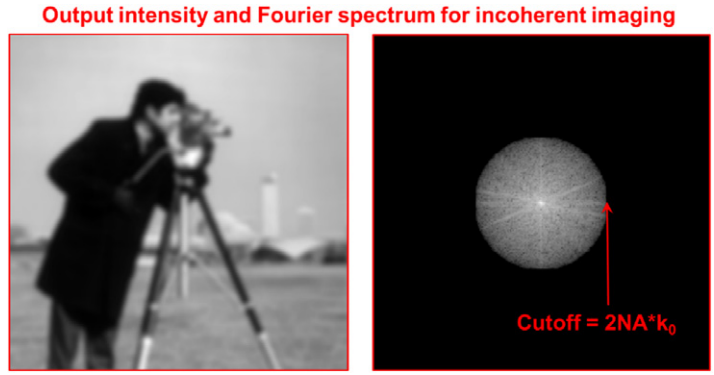


**Figure 1.3.** The simulated output intensity and Fourier spectrum in an incoherent imaging setting.

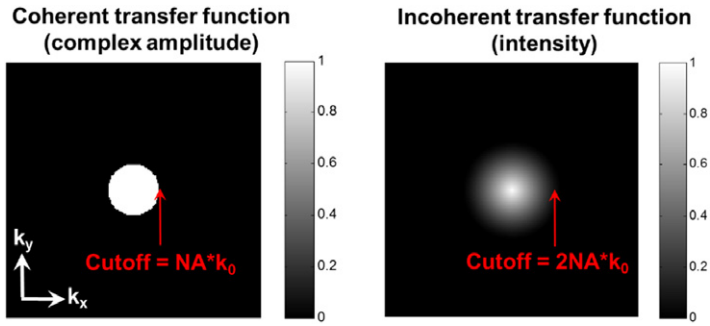


**Figure 1.4.** The comparison between the coherent and incoherent transfer functions.

twice the cutoff frequency of the coherent transfer function. However, it does not follow that incoherent illumination yields a better resolution than coherent illumination, as we are comparing image intensity to complex amplitude. In fact, which type of illumination is better strongly depends on the sample property, and in particular on the phase distribution of the object. The interested reader can refer to chapter 6 in [1] for more details.

## 1.3 Modeling aberrations

In previous sections, we assume the imaging system does not contain any optical aberration. Such a system is called a diffraction-limited system, where the achievable resolution is only determined by the NA. We now consider the effect of optical aberration, which imposes practical limits on resolution performance. In particular, we will model the aberrations using the transfer-function approach. We note that, a treatment of various types of aberrations and their effects on frequency response is beyond the scope of this chapter. The interested reader can refer to, for example, [17].

To model aberrations in the imaging process, we can simply introduce a phase term in the coherent transfer function (CTF) as follows:

$$\mathrm{CTF}\left(k_x, k_y\right) = \mathrm{circ}(NA \cdot k_0) \cdot \mathrm{e}^{\mathrm{i} \cdot W\left(k_x, k_y\right)}, \tag{1.5}$$

where the circle function 'circ' generates a circular mask with a radius of $\mathrm{NA} \cdot k_0$, and $\mathrm{W}(k_x, k_y)$ represents the wavefront aberration of the system. We can further decompose the wavefront aberration into a summation of different Zernike modes $\mathrm{Z}(m, n)$ as follows:

$$\mathrm{W}\left(k_x, k_y\right) = \sum a_{(m,n)} \mathrm{Z}(m, n), \tag{1.6}$$

where $a_{(m,n)}$ represents the coefficient for the Zernike mode $\mathrm{Z}(m, n)$. As an example, we have the second-order defocus aberration $\mathrm{W}(k_x, k_y) = a_{(2,0)}\mathrm{Z}(2, 0)$, where $a_{(2,0)}$ represents the amount of defocus aberration. Similarly, $a_{(2,2)}$ and $a_{(2,-2)}$ represent the amounts of second-order astigmatism aberrations along two directions; $a_{(3,1)}$ and $a_{(3,-1)}$ represent the amounts of third-order coma aberrations along two directions; $a_{(4,0)}$ represents the amount of fourth-order spherical aberration. In short, equations (1.5) and (1.6) provide a means to model different aberrations in the imaging process. In the simulation code, we only need to add the following lines to model them in the coherent transfer function:

```
1  W = 2*gzn(pixelNumber,pixelNumberAperture,2,0)+
       4*gzn(pixelNumber,pixelNumberAperture,4,0);
2  CTF=exp(1i.*W).*((kxm.^2+kym.^2)<cutoffFrequency^2);
3  imshow(angle(CTF),[]);title('Coherent transfer function with aberrations');
```

In line 1, we model the wavefront aberration $\mathrm{W}(k_x, k_y)$ as the summation of the second-order defocus and the fourth-order spherical aberrations. We use the 'gzn' function to generate different Zernike modes (similar Zernike functions can be found on the MATLAB File Exchange site). This function takes four parameters from left to right: the width of the input image, the diameter of the pupil aperture, and the two indexes of the Zernike mode. In particular, we have $a_{(2,0)} = 2$ and $a_{(4,0)} = 4$ in the simulation code. In line 2, we model the coherent transfer function using equation (1.5). Once we get the coherent transfer function with aberrations, we can use the coherent imaging procedures in section 1.1 to obtain the output complex amplitude.

To model aberrations in an incoherent imaging system, we need to convert the coherent transfer function (with aberrations) to the incoherent transfer function using the procedures in section 1.2. We can then apply the incoherent transfer function in the filtering process to generate the output intensity image. In figure 1.5, we show two different aberrations in the Fourier domain and their corresponding coherent and incoherent outputs. We can see that the achievable resolution degrades when wavefront aberrations are presented in the imaging system.

Aberration plays a critical role in the design of an imaging platform. As an example, a conventional microscope has a tradeoff between resolution and field of view. A better resolution usually implies a smaller field of view, limiting the imaging throughput of the microscope platform. The tradeoff between resolution and field of view, in fact, comes from aberrations of the objective lens. The common strategy to expand the field of view is to scale up the lens's size [18]. However, simple

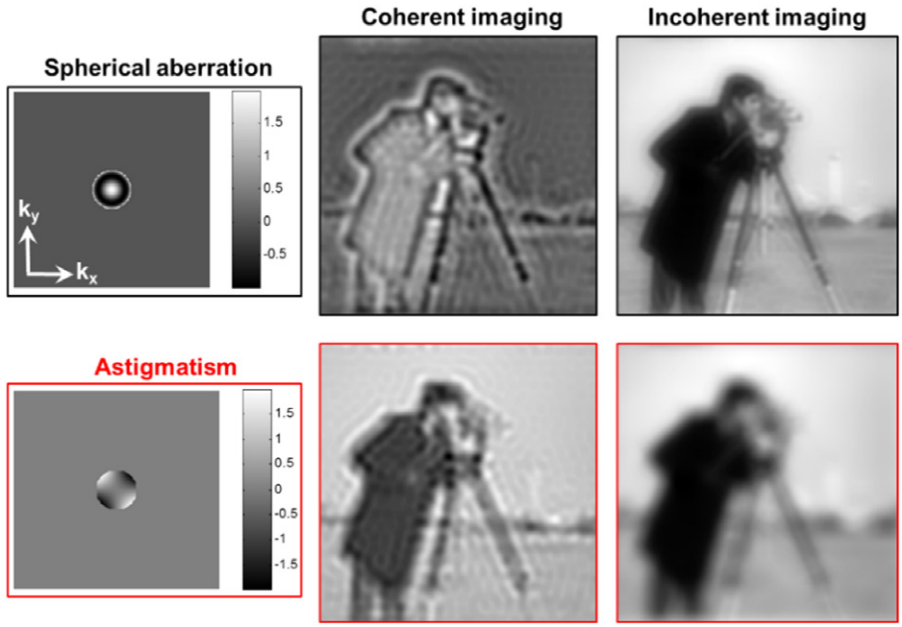


**Figure 1.5.** Modeling aberrations in the coherent and incoherent imaging systems. Top row: the simulated coherent and incoherent images with spherical aberration ($a_{(4,0)}$= 2). Bottom row: the simulated coherent and incoherent images with astigmatism aberration ($a_{(2,2)}$= 4).

size-scaling would introduce aberrations to the system. To compensate for these aberrations, we need to introduce more optical surfaces to increase the degrees of freedom in lens optimization. With the optomechanical constraints of a conventional microscope platform, expanding field of view without compromising the achievable resolution is considered very challenging in the design of high-resolution objective lenses.

## Bibliography

[1] Goodman J W 2005 *Introduction to Fourier optics* (Austin, TX: Roberts and Company)
[2] Goodman J W 2015 *Statistical optics* (Wiley: New York)
[3] Voelz D G 2011 *Computational fourier optics: a MATLAB tutorial* (Bellingham, WA: SPIE Optical Engineering Press)
[4] Fienup J R 1982 Phase retrieval algorithms: a comparison *Appl. Opt.* **21** 2758–69
[5] Elser V 2003 Phase retrieval by iterated projections *JOSA A* **20** 40–55
[6] Faulkner H M L and Rodenburg J M 2004 Movable aperture lensless transmission microscopy: A novel phase retrieval algorithm *Phys. Rev. Lett.* **93** 023903
[7] Maiden A M and Rodenburg J M 2009 An improved ptychographical phase retrieval algorithm for diffractive imaging *Ultramicroscopy* **109** 1256–62
[8] Gonsalves R 1976 Phase retrieval from modulus data *JOSA* **66** 961–4
[9] Fienup J R 1987 Reconstruction of a complex-valued object from the modulus of its Fourier transform using a support constraint *JOSA A* **4** 118–23

[10] Candes E J, Strohmer T and Voroninski V 2013 Phaselift: Exact and stable signal recovery from magnitude measurements via convex programming *Comm. Pure Appl. Math.* **66** 1241–74
[11] Candes E J, Eldar Y C, Strohmer T and Voroninski V 2015 Phase retrieval via matrix completion *SIAM Review* **57** 225–51
[12] Waldspurger I, d'Aspremont A and Mallat S 2015 Phase recovery, maxcut and complex semidefinite programming *Math. Program.* **149** 47–81
[13] Schnars U and Jueptner W 2005 *Digital Holography* (Berlin: Springer)
[14] Cuche E, Marquet P and Depeursinge C 2000 Spatial filtering for zero-order and twin-image elimination in digital off-axis holography *Appl. Opt.* **39** 4070–75
[15] Yamaguchi I and Zhang T 1997 Phase-shifting digital Holography *Opt. Lett.* **22** 1268–70
[16] Zheng G, Horstmeyer R and Yang C 2013 Wide-field, high-resolution Fourier ptychographic microscopy *Nature Photonics* **7** 739–45
[17] Williams C S and Becklund O A 1989 *Introduction to the optical transfer function* vol. 112 (Bellingham, WA: SPIE Optical Engineering Press)
[18] Lohmann A W 1989 Scaling laws for lens systems *Appl. Opt.* **28** 4996–98

# Full list of references

## Chapter 1


[1] Goodman J W 2005 *Introduction to Fourier optics* (Austin, TX: Roberts and Company)
[2] Goodman J W 2015 *Statistical optics* (Wiley: New York)
[3] Voelz D G 2011 *Computational fourier optics: a MATLAB tutorial* (Bellingham, WA: SPIE Optical Engineering Press)
[4] Fienup J R 1982 Phase retrieval algorithms: a comparison *Appl. Opt.* **21** 2758–69
[5] Elser V 2003 Phase retrieval by iterated projections *JOSA A* **20** 40–55
[6] Faulkner H M L and Rodenburg J M 2004 Movable aperture lensless transmission microscopy: A novel phase retrieval algorithm *Phys. Rev. Lett.* **93** 023903
[7] Maiden A M and Rodenburg J M 2009 An improved ptychographical phase retrieval algorithm for diffractive imaging *Ultramicroscopy* **109** 1256–62
[8] Gonsalves R 1976 Phase retrieval from modulus data *JOSA* **66** 961–4
[9] Fienup J R 1987 Reconstruction of a complex-valued object from the modulus of its Fourier transform using a support constraint *JOSA A* **4** 118–23
[10] Candes E J, Strohmer T and Voroninski V 2013 Phaselift: Exact and stable signal recovery from magnitude measurements via convex programming *Comm. Pure Appl. Math.* **66** 1241–74
[11] Candes E J, Eldar Y C, Strohmer T and Voroninski V 2015 Phase retrieval via matrix completion *SIAM Review* **57** 225–51
[12] Waldspurger I, d'Aspremont A and Mallat S 2015 Phase recovery, maxcut and complex semidefinite programming *Math. Program.* **149** 47–81
[13] Schnars U and Jueptner W 2005 *Digital Holography* (Berlin: Springer)
[14] Cuche E, Marquet P and Depeursinge C 2000 Spatial filtering for zero-order and twin-image elimination in digital off-axis holography *Appl. Opt.* **39** 4070–75
[15] Yamaguchi I and Zhang T 1997 Phase-shifting digital Holography *Opt. Lett.* **22** 1268–70
[16] Zheng G, Horstmeyer R and Yang C 2013 Wide-field, high-resolution Fourier ptychographic microscopy *Nature Photonics* **7** 739–45
[17] Williams C S and Becklund O A 1989 *Introduction to the optical transfer function* vol. 112 (Bellingham, WA: SPIE Optical Engineering Press)
[18] Lohmann A W 1989 Scaling laws for lens systems *Appl. Opt.* **28** 4996–98


## Chapter 2


[1] Lohmann A W, Dorsch R G, Mendlovic D, Zalevsky Z and Ferreira C 1996 Space-bandwidth product of optical signals and systems *JOSA A* **13** 470–3
[2] Zheng G, Horstmeyer R and Yang C 2013 Wide-field, high-resolution Fourier ptychographic microscopy *Nat. Photonics* **7** 739–45
[3] Zheng G, Ou X, Horstmeyer R, Chung J and Yang C 2014 Fourier Ptychographic Microscopy: A Gigapixel Superscope for Biomedicine *Opt. and Photonics News* 26–33
[4] Zheng G 2014 Breakthroughs in Photonics 2013: Fourier Ptychographic Imaging *Photonics Journal, IEEE* **6** 1–7
[5] Fienup J R 1982 Phase retrieval algorithms: a comparison *Appl. Opt.* **21** 2758–69
[6] Elser V 2003 Phase retrieval by iterated projections *JOSA A* **20** 40–55

[7] Faulkner H M L and Rodenburg J M 2004 Movable Aperture Lensless Transmission Microscopy: A Novel Phase Retrieval Algorithm *Phys. Rev. Lett.* **93** 023903
[8] Maiden A M and Rodenburg J M 2009 An improved ptychographical phase retrieval algorithm for diffractive imaging *Ultramicroscopy* **109** 1256–62
[9] Gonsalves R 1976 Phase retrieval from modulus data *JOSA* **66** 961–4
[10] Fienup J R 1987 Reconstruction of a complex-valued object from the modulus of its Fourier transform using a support constraint *JOSA A* **4** 118–23
[11] Candes E J, Strohmer T and Voroninski V 2013 Phaselift: Exact and stable signal recovery from magnitude measurements via convex programming *Comm. Pure Appl. Math.* **66** 1241–74
[12] Candes E J, Eldar Y C, Strohmer T and Voroninski V 2015 Phase retrieval via matrix completion *SIAM Review* **57** 225–51
[13] Waldspurger I, d'Aspremont A and Mallat S 2015 Phase recovery, maxcut and complex semidefinite programming *Math. Program.* **149** 47–81
[14] Mico V, Zalevsky Z, García-Martínez P and García J 2006 Synthetic aperture super-resolution with multiple off-axis holograms *JOSA A* **23** 3162–70
[15] Di J, Zhao J, Jiang H, Zhang P, Fan Q and Sun W 2008 High resolution digital holographic microscopy with a wide field of view based on a synthetic aperture technique and use of linear CCD scanning *Appl. Opt.* **47** 5654–9
[16] Hillman T R, Gutzler T, Alexandrov S A and Sampson D D 2009 High-resolution, wide-field object reconstruction with synthetic aperture Fourier holographic optical microscopy *Opt. Exp.* **17** 7873–92
[17] Granero L, Micó V, Zalevsky Z and García J 2010 Synthetic aperture superresolved microscopy in digital lensless Fourier holography by time and angular multiplexing of the object information *Appl. Opt.* **49** 845–57
[18] Gutzler T, Hillman T R, Alexandrov S A and Sampson D D 2010 Coherent aperture-synthesis, wide-field, high-resolution holographic microscopy of biological tissue *Opt. Lett.* **35** 1136–8
[19] Meinel A 1970 Aperture synthesis using independent telescopes *Appl. Opt.* **9** 2501
[20] Turpin T, Gesell L, Lapides J and Price C 1995 Theory of the synthetic aperture microscope *Proc. SPIE* **2566** 230–40
[21] Ryle M and Hewish A 1960 The synthesis of large radio telescopes *Mon. Not. R. Astron. Soc.* **120** 220
[22] Hillman T R, Gutzler T, Alexandrov S A and Sampson D D 2009 High-resolution, wide-field object reconstruction with synthetic aperture Fourier holographic optical microscopy *Opt. Exp.* **17** 7873–92
[23] Kim M, Choi Y, Fang-Yen C, Sung Y, Dasari R R and Feld M S *et al* 2011 High-speed synthetic aperture microscopy for live cell imaging *Opt. Lett.* **36** 148–50
[24] Schwarz C J, Kuznetsova Y and Brueck S 2003 Imaging interferometric microscopy *Opt. Lett.* **28** 1424–26
[25] Feng P, Wen X and Lu R 2009 Long-working-distance synthetic aperture Fresnel off-axis digital holography *Opt. Exp.* **17** 5473–80
[26] Yuan C, Zhai H and Liu H 2008 Angular multiplexing in pulsed digital holography for aperture synthesis *Opt. Lett.* **33** 2356–8
[27] Mico V, Zalevsky Z and García J 2007 Synthetic aperture microscopy using off-axis illumination and polarization coding *Opt. Comm.* **276** 209–17

[28] Alexandrov S and Sampson D 2008 Spatial information transmission beyond a system's diffraction limit using optical spectral encoding of the spatial frequency *J. Optics A: Pure and Appl. Opt.* **10** 025304
[29] Tippie A E, Kumar A and Fienup J R 2011 High-resolution synthetic-aperture digital holography with digital phase and pupil correction *Opt. Exp.* **19** 12027–38
[30] Alexandrov S A, Hillman T R, Gutzler T and Sampson D D 2006 Synthetic aperture Fourier holographic optical microscopy *Phys. Rev. Lett.* **97** 168102
[31] Ou X, Horstmeyer R, Yang C and Zheng G 2013 Quantitative phase imaging via Fourier ptychographic microscopy *Opt. Lett.* **38** 4845–8
[32] Guizar-Sicairos M and Fienup J R 2008 Phase retrieval with transverse translation diversity: a nonlinear optimization approach *Opt. Exp.* **16** 7264–78
[33] Li P, Batey D J, Edo T B and Rodenburg J M 2015 Separation of three-dimensional scattering effects in tilt-series Fourier ptychography *Ultramicroscopy* **158** 1–7
[34] Hoppe W and Strube G 1969 Diffraction in inhomogeneous primary wave fields. 2. Optical experiments for phase determination of lattice interferences *Acta Crystallogr.* A **25** 502–7
[35] Rodenburg J, Hurst A, Cullis A, Dobson B, Pfeiffer F and Bunk O *et al* 2007 Hard-x-ray lensless imaging of extended objects *Phys. Rev. Lett.* **98** 034801
[36] Rodenburg J 2008 Ptychography and related diffractive imaging methods *Adv. Imag. Electr. Phys.* **150** 87
[37] Horstmeyer R and Yang C 2014 A phase space model of Fourier ptychographic microscopy *Opt. Exp.* **22** 338–58
[38] Ou X, Zheng G and Yang C 2014 Embedded pupil function recovery for Fourier ptychographic microscopy *Opt. Exp.* **22** 4960–72
[39] Bian Z, Dong S and Zheng G 2013 Adaptive system correction for robust Fourier ptychographic imaging *Opt. Exp.* **21** 32400–10
[40] Dong S, Guo K, Nanda P, Shiradkar R and Zheng G 2014 FPscope: a field-portable high-resolution microscope using a cellphone lens *Biomed. Opt. Exp.* **5** 3305–10
[41] Guo K, Dong S, Nanda P and Zheng G 2015 Optimization of sampling pattern and the design of Fourier ptychographic illuminator *Opt. Exp.* **23** 6171–80
[42] Bian L, Suo J, Situ G, Zheng G, Chen F and Dai Q 2014 Content adaptive illumination for Fourier ptychography *Opt. Lett.* **39** 6648–51
[43] Huang X, Yan H, Harder R, Hwu Y, Robinson I K and Chu Y S 2014 Optimization of overlap uniformness for ptychography *Opt. Exp.* **22** 12634–44
[44] Dong S, Horstmeyer R, Shiradkar R, Guo K, Ou X and Bian Z *et al* 2014 Aperture-scanning Fourier ptychography for 3D refocusing and super-resolution macroscopic imaging *Opt. Exp.* **22** 13586–99
[45] Levoy M, Ng R, Adams A, Footer M and Horowitz M 2006 Light field microscopy *ACM Transactions on Graphics* **25** 924–34
[46] Levoy M, Zhang Z and McDowall I 2009 Recording and controlling the 4D light field in a microscope using microlens arrays *J. Microsc.* **235** 144–62
[47] Zheng G, Kolner C and Yang C 2011 Microscopy refocusing and dark-field imaging by using a simple LED array *Opt. Lett.* **36** 3987–9
[48] Thibault P, Dierolf M, Bunk O, Menzel A and Pfeiffer F 2009 Probe retrieval in ptychographic coherent diffractive imaging *Ultramicroscopy* **109** 338–43
[49] Dong S, Bian Z, Shiradkar R and Zheng G 2014 Sparsely sampled Fourier ptychography *Opt. Exp.* **22** 5455–64

[50] Edo T B, Batey D J, Maiden A M, Rau C, Wagner U and Pešić Z D *et al* 2013 Sampling in x-ray ptychography *Phys. Rev.* A **87** 053850
[51] Dong S, Shiradkar R, Nanda P and Zheng G 2014 Spectral multiplexing and coherent-state decomposition in Fourier ptychographic imaging *Biomedical Opt. Exp.* **5** 1757–67
[52] Thibault P and Menzel A 2013 Reconstructing state mixtures from diffraction measurements *Nature* **494** 68–71
[53] Batey D J, Claus D and Rodenburg J M 2014 Information multiplexing in ptychography *Ultramicroscopy* **138** 13–21

## Chapter 3

[1] Zheng G, Kolner C and Yang C 2011 Microscopy refocusing and dark-field imaging by using a simple LED array *Opt. Lett.* **36** 3987–9
[2] Zheng G 2012 Microscopy-Programmable LED array makes microscopes more versatile *Laser Focus World* **48** 66
[3] Zheng G, Horstmeyer R and Yang C 2013 Wide-field, high-resolution Fourier ptychographic microscopy *Nature Photonics* **7** 739–45
[4] Ou X, Horstmeyer R, Zheng G and Yang C 2015 High numerical aperture Fourier ptychography: principle, implementation and characterization *Opt. Exp.* **23** 3472–91
[5] Thibault P, Dierolf M, Bunk O, Menzel A and Pfeiffer F 2009 Probe retrieval in ptychographic coherent diffractive imaging *Ultramicroscopy* **109** 338–43
[6] Guo K, Dong S, Nanda P and Zheng G 2015 Optimization of sampling pattern and the design of Fourier ptychographic illuminator *Opt. Exp.* **23** 6171–80
[7] Dong S, Guo K, Nanda P, Shiradkar R and Zheng G 2014 FPscope: a field-portable high-resolution microscope using a cellphone lens *Biomed. Opt. Exp.* **5** 3305–10
[8] Guo K, Bian Z, Dong S, Nanda P, Wang Y M and Zheng G 2015 Microscopy illumination engineering using a low-cost liquid crystal display *Biomed. Opt. Exp.* **6** 574–9
[9] Dong S, Horstmeyer R, Shiradkar R, Guo K, Ou X and Bian Z *et al* 2014 Aperture-scanning Fourier ptychography for 3D refocusing and super-resolution macroscopic imaging *Opt. Exp.* **22** 13586–99
[10] Luo W, Greenbaum A, Zhang Y and Ozcan A 2015 Synthetic aperture-based on-chip microscopy *Light: Science & Applications* **4** e261
[11] Sidorenko P and Cohen O 2016 Single-shot ptychography *Optica* **3** 9–14
[12] Ou X, Horstmeyer R, Yang C and Zheng G 2013 Quantitative phase imaging via Fourier ptychographic microscopy *Opt. Lett.* **38** 4845–8
[13] Mir M, Tangella K and Popescu G 2011 Blood testing at the single cell level using quantitative phase and amplitude microscopy *Biomed. Opt. Exp.* **2** 3259
[14] Kim T, Sridharan S, Kajdacsy-Balla A, Tangella K and Popescu G 2013 Gradient field microscopy for label-free diagnosis of human biopsies *Appl. Opt.* **52** A92–A96
[15] Wang Z, Tangella K, Balla A and Popescu G 2011 Tissue refractive index as marker of disease *J. Biomed. Opt.* **16** 116017–177
[16] Zheng G 2014 Breakthroughs in Photonics 2013: Fourier Ptychographic Imaging *Photonics J. IEEE* **6** 1–7
[17] Guo K, Dong S and Zheng G 2016 Fourier Ptychography for Brightfield, Phase, Darkfield, Reflective, Multi-slice, and Fluorescence Imaging, *IEEE J. Select. Topics Quant. Electr.* at press

[18] Pacheco S, Zheng G and Liang R 2016 Reflective Fourier ptychography *J. Biomed. Opt.* **21** 026010
[19] Maiden A M, Humphry M J and Rodenburg J M 2012 Ptychographic transmission microscopy in three dimensions using a multi-slice approach *J. Opt. Soc. Am.* **29** 1606–14
[20] Godden T, Suman R, Humphry M, Rodenburg J and Maiden A 2014 Ptychographic microscope for three-dimensional imaging *Opt. Exp.* **22** 12513
[21] Li P, Batey D J, Edo T B and Rodenburg J M 2015 Separation of three-dimensional scattering effects in tilt-series Fourier ptychography *Ultramicroscopy* **158** 1–7
[22] Tian L and Waller L 2015 3D intensity and phase imaging from light field measurements in an LED array microscope *Optica* **2** 104–11
[23] Sheppard C J R and Cogswell C J 1990 Three-dimensional image formation in confocal microscopy *J. Microsc.* **159** 179–94

## Chapter 4

[1] Dong S, Nanda P, Shiradkar R, Guo K and Zheng G 2014 High-resolution fluorescence imaging via pattern-illuminated Fourier ptychography *Opt. Exp.* **22** 20856–70
[2] Chakrova N, Heintzmann R, Rieger B and Stallinga S 2015 Studying different illumination patterns for resolution improvement in fluorescence microscopy *Opt. Exp.* **23** 31367–83
[3] Dong S, Liao J, Guo K, Bian L, Suo J and Zheng G 2015 Resolution doubling with a reduced number of image acquisitions *Biomed. Opt. Exp.* **6** 2946–52
[4] Dong S, Guo K, Jiang S and Zheng G 2015 Recovering higher dimensional image data using multiplexed structured illumination *Opt. Exp.* **23** 30393–8
[5] Dong S, Nanda P, Guo K, Liao J and Zheng G 2015 Incoherent Fourier ptychographic photography using structured light *Photonics Res.* **3** 19–23
[6] Gustafsson M G 2000 Surpassing the lateral resolution limit by a factor of two using structured illumination microscopy *J. Microsc.* **198** 82–7
[7] Gustafsson M G 2005 Nonlinear structured-illumination microscopy: wide-field fluorescence imaging with theoretically unlimited resolution *Proc. Natl Acad. Sci. USA* **102** 13081–6
[8] Gustafsson M G, Shao L, Carlton P M, Wang C, Golubovskaya I N and Cande W Z *et al* 2008 Three-dimensional resolution doubling in wide-field fluorescence microscopy by structured illumination *Biophys. J.* **94** 4957–70
[9] Heintzmann R and Gustafsson M G 2009 Subdiffraction resolution in continuous samples *Nat. Photonics* **3** 362–4
[10] Kner P, Chhun B B, Griffis E R, Winoto L and Gustafsson M G 2009 Super-resolution video microscopy of live cells by structured illumination *Nat. Methods* **6** 339–42
[11] Mudry E, Belkebir K, Girard J, Savatier J, Le Moal E and Nicoletti C *et al* 2012 Structured illumination microscopy using unknown speckle patterns *Nat. Photonics* **6** 312–5
[12] Jost A and Heintzmann R 2013 Superresolution multidimensional imaging with structured illumination microscopy *Annual Rev. Mater. Res.* **43** 261–82
[13] Min J, Jang J, Keum D, Ryu S-W, Choi C and Jeong K-H *et al* 2013 Fluorescent microscopy beyond diffraction limits using speckle illumination and joint support recovery *Scientific Reports* **3**
[14] So P T C, Kwon H-S and Dong C Y 2001 Resolution enhancement in standing-wave total internal reflection microscopy: a point-spread-function engineering approach *J. Opt. Soc. Am.* **18** 2833–45

[15] Ou X, Zheng G and Yang C 2014 Embedded pupil function recovery for Fourier ptychographic microscopy *Opt. Exp.* **22** 4960–72
[16] Gustafsson M G, Shao L, Carlton P M, Wang C R, Golubovskaya I N and Cande W Z *et al* 2008 Three-dimensional resolution doubling in wide-field fluorescence microscopy by structured illumination *Biophys. J.* **94** 4957–70
[17] Thibault P and Menzel A 2013 Reconstructing state mixtures from diffraction measurements *Nature* **494** 68–71
[18] Batey D J, Claus D and Rodenburg J M 2014 Information multiplexing in ptychography *Ultramicroscopy* **138** 13–21

## Chapter 5

[1] Horstmeyer R, Ou X, Zheng G, Willems P and Yang C 2015 Digital pathology with Fourier ptychography *Comput. Med. Imaging Graph.* **42** 38–43
[2] Williams A, Chung J, Ou X, Zheng G, Rawal S and Ao Z *et al* 2014 Fourier ptychographic microscopy for filtration-based circulating tumor cell enumeration and analysis *J. Biomed. Opt.* **19** 066007
[3] Chung J, Ou X, Kulkarni R P and Yang C 2015 Counting white blood cells from a blood smear using fourier ptychographic microscopy *PloS one* **10**
[4] Zheng G, Ou X, Horstmeyer R, Chung J and Yang C 2014 Fourier Ptychographic Microscopy: A Gigapixel Superscope for Biomedicine *Opt. Photonics News* April Issue 26–33
[5] Ou X, Horstmeyer R, Yang C and Zheng G 2013 Quantitative phase imaging via Fourier ptychographic microscopy *Opt. Lett.* **38** 4845–8
[6] Guo K, Dong S and Zheng G 2016 Fourier Ptychography for Brightfield, Phase, Darkfield, Reflective, Multi-slice, and Fluorescence Imaging *IEEE J. Select. Topics Quant. Electr.* at press
[7] Pacheco S, Zheng G and Liang R 2016 Reflective Fourier ptychography *J. Biomed. Opt.* **21** 026010
[8] Bian Z, Dong S and Zheng G 2013 Adaptive system correction for robust Fourier ptychographic imaging *Opt. Exp.* **21** 32400–10
[9] Ou X, Zheng G and Yang C 2014 Embedded pupil function recovery for Fourier ptychographic microscopy *Opt. Exp.* **22** 4960–72
[10] Konda P C, Taylor J M and Harvey A R 2015 High-resolution microscopy with low-resolution objectives: correcting phase aberrations in Fourier ptychography in *SPIE* 96300X–8
[11] Dong S, Horstmeyer R, Shiradkar R, Guo K, Ou X and Bian Z *et al* 2014 Aperture-scanning Fourier ptychography for 3D refocusing and super-resolution macroscopic imaging *Opt. Exp.* **22** 13586–99
[12] Dong S, Nanda P, Shiradkar R, Guo K and Zheng G 2014 High-resolution fluorescence imaging via pattern-illuminated Fourier ptychography *Opt. Exp.* **22** 20856–70
[13] Dong S, Liao J, Guo K, Bian L, Suo J and Zheng G 2015 Resolution doubling with a reduced number of image acquisitions *Biomed. Opt. Exp.* **6** 2946–52
[14] Dong S, Guo K, Jiang S and Zheng G 2015 Recovering higher dimensional image data using multiplexed structured illumination *Opt. Exp.* **23** 30393–8
[15] Thibault P and Menzel A 2013 Reconstructing state mixtures from diffraction measurements *Nature* **494** 68–71

[16] Batey D J, Claus D and Rodenburg J M 2014 Information multiplexing in ptychography *Ultramicroscopy* **138** 13–21
[17] Dong S, Shiradkar R, Nanda P and Zheng G 2014 Spectral multiplexing and coherent-state decomposition in Fourier ptychographic imaging *Biomed. Opt. Exp.* **5** 1757–67
[18] Tian L, Li X, Ramchandran K and Waller L 2014 Multiplexed coded illumination for Fourier Ptychography with an LED array microscope *Biomed. Opt. Exp.* **5** 2376–89
[19] Maiden A M, Humphry M J and Rodenburg J M 2012 Ptychographic transmission microscopy in three dimensions using a multi-slice approach *J. Opt. Soc. America* A **29** 1606–14
[20] Godden T, Suman R, Humphry M, Rodenburg J and Maiden A 2014 Ptychographic microscope for three-dimensional imaging *Opt. Exp.* **22** 12513
[21] Li P, Batey D J, Edo T B and Rodenburg J M 2015 Separation of three-dimensional scattering effects in tilt-series Fourier ptychography *Ultramicroscopy* **158** 1–7
[22] Tian L and Waller L 2015 3D intensity and phase imaging from light field measurements in an LED array microscope *Optica* **2** 104–11
[23] Sidorenko P and Cohen O 2016 Single-shot ptychography *Optica* **3** 9–14
[24] Dong S, Nanda P, Guo K, Liao J and Zheng G 2015 Incoherent Fourier ptychographic photography using structured light *Photonics Res.* **3** 19–23
[25] Guo K, Liao J, Bian Z, Heng X and Zheng G 2015 InstantScope: a low-cost whole slide imaging system with instant focal plane detection *Biomed. Opt. Exp.* **6** at press